



A BIOMIMETIC UNDERWATER ROBOT DIRECTION CHANGING ALGORITHMS

AFOLAYAN Matthew Olatunde

Mechanical Engineering Department, Ahmadu Bello University, Zaria, Nigeria

*Corresponding authors' email: tunde_afolayan@yahoo.com
ORCID: 0000-0003-3426-1383

ABSTRACT

The performance of the steady-turning while swimming, and sharp-turning motion algorithms of a biomimetic underwater robot in the form of a fish is presented in this work. The biological fish modelled is a Mackerel - *Scomber scombrus*. Its motion patterns are precalculated and programmed into its firmware as an inflexible algorithm to save power consumption due to continuous motor position recalculations. The robot tail is a six segments plywood panels with vulcanized rubber acting as joints. This tail structure is driven by three remote-control servomotors (Futaba 3003) under the control of microcontroller (PIC18F4520). The algorithm for steady turning is derived steady swimming by introducing offset in the servomotor displacements about the midline of the robot. The algorithm for sharp turning treats the three servomotors as one and turn them simultaneously to left or right and restore them quickly into straight form, which allows the robot to turn at a tight corner. A 54cm turning radius was achieved with the steady turn while swimming, this will allow the robot to turn in a tight corner and crevices. The sharp turn however works but requires several attempts before a proper reorientation was achieved in the desired direction.

Keywords: Biomimicry, Hyper-Redundant, Robotic fish, Swimming, *Teleost* sp., Turning

INTRODUCTION

Water, covers more than 70% of our planet, meaning 70% of the earth natural resources is perhaps locked there as well as a huge number of unknown plants and animals' species and human history. "Underwater environment is one of the most difficult places for man to be in" according to Salumäe (2014). The main reason is because of the extreme hydrostatic pressure existing in the ocean due to the density and depth of water - which is above what human-being can tolerate. The maximum recommended technical diving limit using the most advanced technology is only 100 m according to Salumäe (2014). Any diving beyond this requires the use of diving tube with proper climate control inside it. A US navy diver was able to get to a depth of 610 m (Logico, 2006) using such device and furthermore, in 2012, James Cameron went down 10.94 km deep into Marianna Trench using a submersible (Than, 2012). This progress made so far covers very small portion of our world under the water. Thus, unaided or without special vehicles, most of the underwater world (70% of our world) will remain unexplorable. Underwater robots provide an engineering tool to practical applications in marine and military fields, such as monitoring the environment, harvesting natural resources, undersea operation, pipe inspection, telecoms submersible cable inspection and many more applications (Daou *et al.*, 2012; Mark, 2021). This is similar to what the works of Salisu and Shallah (2020) and Martins *et al.* (2019) aimed to achieve ultimately in terms of robot use for security, human replacement etc on the terra firma.

Most of marine and underwater mechanisms, such as ships, submarines, or underwater robots use screw propellers for propulsion. Although these devices work sufficiently well for most purposes, the systems designed by nature still outperform them. Fishes are well known efficient swimmer when compared to man-made under water vehicles. In comparison, efficiency of fish swimming can be as high as 97% (Müller, 1997), while efficiency of propellers does not generally exceed 70% (Watson, 2000), they are quiet when swimming, they can make a very rapid and sharp turnings not possible with any man-made UAV system. Their acceleration is with lightning speed (Jindong and Huosheng, 2007; Li, *et al.*, 2018; NMRI, 2020). Fish can maneuver in complex environments with lots of different species of animals, these abilities make it easier for

them to escape predators (Marchese *et al.*, 2014) These capabilities is inspirational for designing new kind of propulsion mechanisms (Salumäe and Kruusmaa, 2011).

Fish swims using either of these two fundamental modes, use of the whole body as in Body and/or Caudal Fin (BCF) locomotion (for high-speed motions) or Median and/or Paired Fin (MPF) (Breder, 1926; Sfakiotakis *et al.*, 1999) locomotion (for fishes that needs to move slowly and at much more efficiency) (Yangwei *et al.*, 2015). It is known that fishes use vortex around them to aid their efficient swimming (Anderson, 1996; Streitlien *et al.*, 1996; Wang *et al.*, 2010). *Teleost* species of fishes such as Mackerel use BCF locomotion system. Furthermore, fishes swim in different configurations, such as straight wiggling motion, sharp turning, steady turning, diving, surfing (going to surface), gliding as in Sailfish, lateral undulation, sinus lifting, sidewarding, and climbing, etc (Afolayan and Iorpenda, 2021)

An underwater robot in the form of a fish belongs to a class of robot known as biomimetic robots – biologically inspired robots. Biologically inspired robots imitate some characteristics of life forms such as mobility, vision, flying and navigational methodology. Biomimetic systems are greatly desired because natural systems are highly optimized and efficient. Srinivasan (1992) and Salumäe (2014) described them as possessing shortcuts to mathematically complex issues of control in real life scenario. Furthermore, underwater robot in the form of a fish structurally belong to hyper-redundant bodies since they possess several joints. A hyper-redundant robot has the following advantages; their redundancy allows them to still function after losing mobility in one or more sections, stability in all terrain because of low center of gravity, small tubular size that can penetrate small crevices and thus useful for search and rescue among rubbles and convoluted or clustered environments, high efficiency in energy use as there is no need to lift the body. Also, they can be made amphibious, the same body motion used for swimming in water is also used for moving on land.

However, robots having hyper-redundant joints have these problems; how to control, programme and build an efficient control system for the several degrees of freedom (DOF) links or joints. Furthermore, they have (i) low speed as the whole body is used for motion (ii) poor thermal control because of

low surface to volume ratio, (iii) design implementation (Kevin, 1997; Shugen and Mitsuru, 2002; Andrés *et al.*, 2020). This study is about the algorithms for steady-turning while swimming and sharp-turning (or C-turning) developed for a Mackerel (*Scomber scombrus*) based robotic fish. It uses an inflexible but less computational demanding design called built-in patterns for its motor and motion control scheme, because being an untethered device, it will have to run on battery, and there is need to save power consumption due to continuous motor position recalculations. The design could be suitable for other robotic fishes imitating *Teleost* species of fishes such as Herring, Pike, Carp, Cod, Salmon, Bonito, Tuna, and Sword Fish. *Teleost* species of fish are the fastest moving creature inside the water and imitating them will be a step further into designing an efficient and fast underwater system.

MATERIALS AND METHODS

Design description of the robotic fish mechanism

A brief description of the robot (Afolayan *et al.*, 2012) for which the algorithm was developed for is given here. Using the

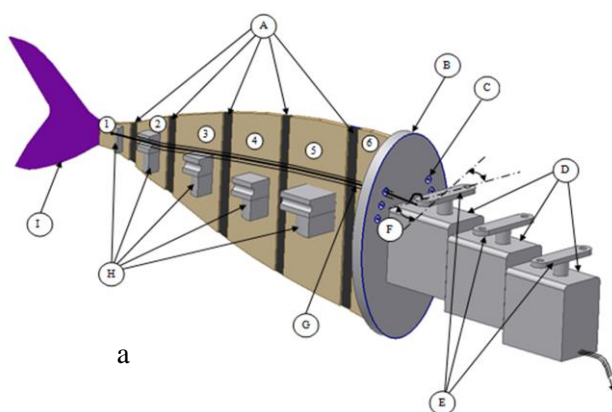
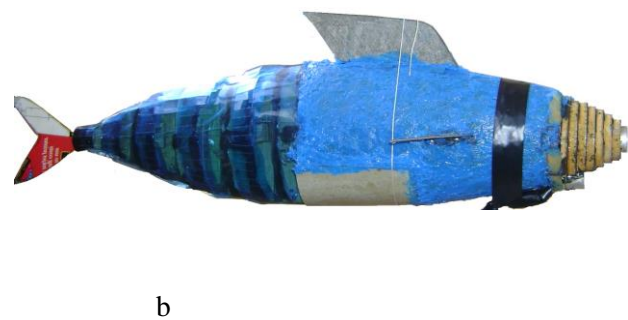


Figure 1: (a) 3D CAD model of the robot

3D CAD model of the robot tail, Figure 1, the tail, consisting of 1.5 mm thick vulcanized rubber joint (A) is sandwiched between pairs of rigid support segments (1) to (6) made from 3.2 mm thick seasoned plywood. The support (6) is attached to oval support (B) having six pass-through holes (C) for the cables support. The servomotor (Futaba 3003) (D) is attached to the oval support (B) having pass-through holes for the cables. The cables are connected to the servomotor lever (E). The microcontroller (PIC18F4520) controls the sequence of turning of the servomotors (D) and hence the segments (1), (3), and (5) they are connected to with the nylon cables. It sends the angular displacement information to the servomotors in such a manner that its lever (E) will oscillate at \pm angle (F). On both sides of each segment (1) to (6) is located quarter pulleys (H) (made from 19 mm thick plywood) over which the 0.5 mm diameter nylon cable (G) passes before hooking to those segments, only one cable is shown for clarity.



(b) the assembled robot

The design description of the robot motor controller

The flow chart for the robot motor control is as shown in Figure 2, it is a firmware-based Pulse-Width-Modulation (PWM) signal generator for 3 rigidly coupled motors. It is based on Microchip PIC18F4520 instruction set, running at 8MIP (32Mhz). The flow chart is divided into 4 sections; Section A is the time base, it uses Timer0 (INT0) interrupt set to trigger repetitively at 20ms interval. The targeted servomotor is Futaba RC servomotor and it requires a 20ms data refresh rate. The length of each pulse determines the angular displacement of each servomotor lever. Section B is where the pulse length data and phase data exist (both data comes in pairs – one for left motion of the robot peduncle and the other for the right motion of the robot peduncle), and what value to load into the duty cycle RAM is determined and manipulated by internal and external inputs. Section C generates the PWM whose duty cycles are based on the inputs from section B. RD0, RD1 and RD2 are the outputs terminal that drives the servomotors. Section D keeps a record of the current state of the ports (1,2,3) so that it can be regenerated again or used as a reference for the next data to be loaded into

section B. For phase difference generation among the motors, the pulse lengths data are retrieved from a table of pre-calculated values hardcoded into the firmware, and each value corresponds to from 1ms to 2ms long (0° to 180°) when loaded into the PWM generator, 1.5ms long pulse translates to 90° turn of the servomotor lever. The pulse lengths data are retrieved during the idle time of the microcontroller. The values are selected such that the motor levers are turned to different angles that are out of phase at any point in time as shown in Figure 3. This is what is called built-in pattern generation, it reduces computational burdens which reduces the amount of clock period to get a result out, thus lesspower is consumed. To generate a different duty cycle for each servomotor, the three ports are first set high by the Timer0. A counting up routine (Section C of Figure 2) is then initiated by looping (sequentially for each port data) until the value is equal to or greater than the retrieved value. This leads to the port (that met the criteria) being set low (to vss). Other ports remain high until set low, thus generating the specified pulse lengths which translate to the duty cycle as desired which makes the phase remains different as shown in figure 3.

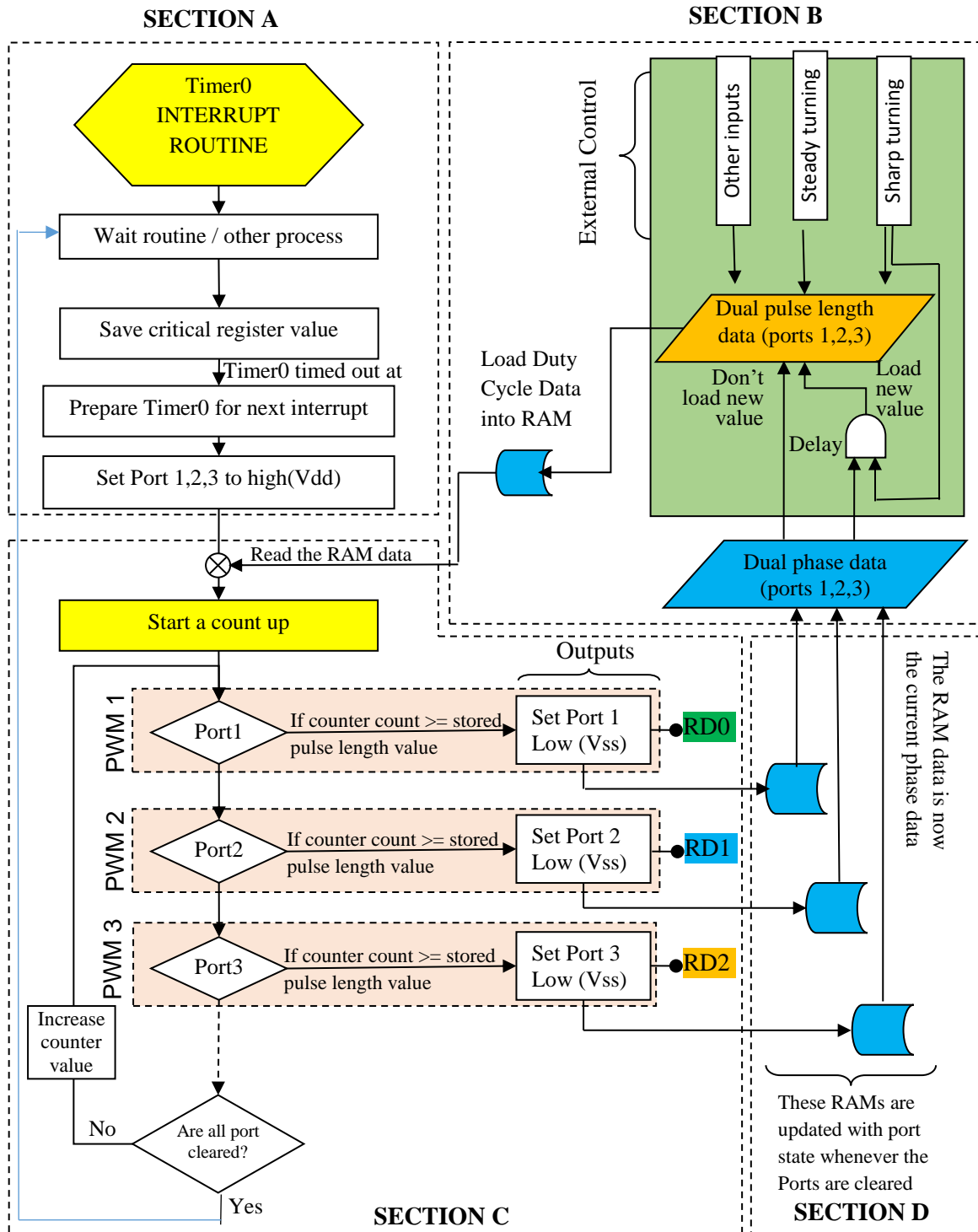


Figure 2: Flow chart of the PWM generator

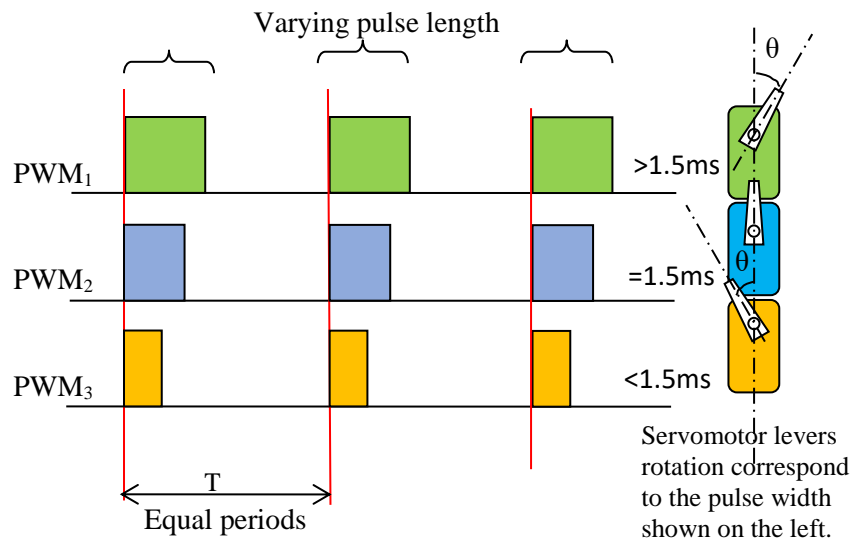


Figure 3: Phase Generation with three servomotors

How Teleost sp of fish swimming is imitated

As pointed out in the introductory section, fishes swim using different body motions. Mackerel (and other teleost fishes) swim by generating a traveling wave such that the amplitude is least at the beginning (towards the head) and is highest at the fin tip/ peduncle (Figure 4a and 4c). In this work, the six links implementation in the robot (Figure 1) is approximated by three links configurations as shown in Figure 4b. The rubber joints allow the shape to be closer to the desired pattern required for swimming and also for restoring the links to straight shape.

This work is focusing on Teleost sp of fish implementation of BCF motion and specifically on turning algorithms (steady-turning while swimming and sharp-turning (or C-turning) developed for a Mackerel (*Scomber scombrus*) based robotic fish. These two motions will be expanded on.

Algorithm for steady-turning while swimming

In this swimming mode, the robotic fish motion steadily deviates from a straight line to the left or right. The turning is first initiated by human control interface or some built in sensors (e.g bump sensors (Afolayan *et al.*, 2014). The turning is done by restraining the motion of the tail such that its excursion on both sides of the fish midline is not equal in amplitude. A lopsided traveling wave (Figure 5) is created when swimming, which induce a turning moment to the motion of the robot. The amplitude on the side it is turning away from is less than that it is turning towards. One of the paired data used for normal swimming, is needed to achieve the turning. In Figure 6, if turning towards left, the pulse width length is set at 1.5ms (for the maximum) and the minimum amplitude is unchanged. If turning towards right, the pulse width length is set at 1.5ms (for the minimum) and the maximum amplitude is unchanged. The 1.5ms pulse width is approximately the pulse width required for the servomotor lever to turn to the middle, which is 90°.

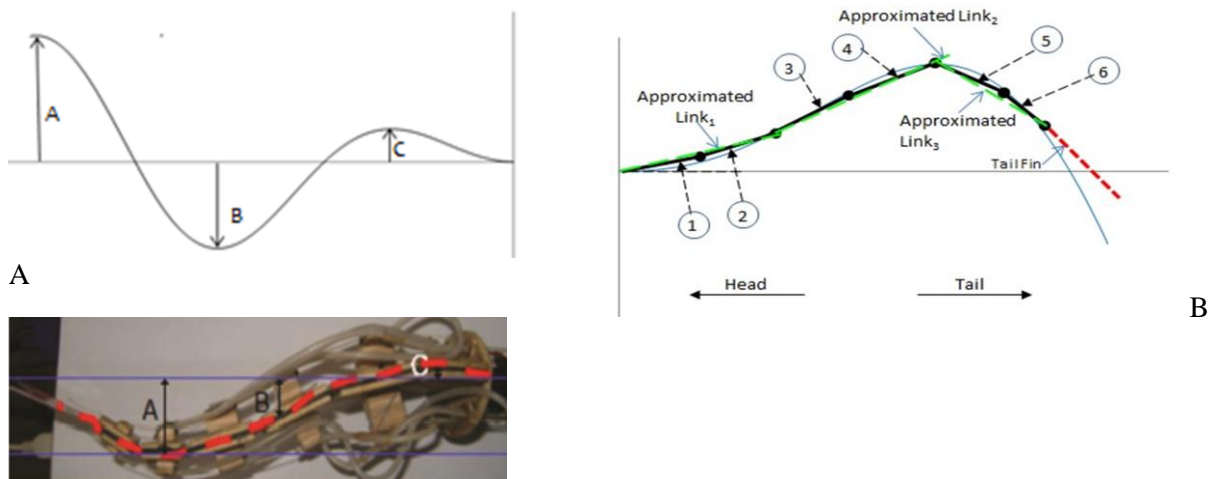


Figure 4: Teleost fish swimming pattern – (a) Tail amplitude increases toward the tail fin, such that the amplitude at $A < B < C$ all the time. (b) The six links (1) – (6) (black colour) implementation in the robot is approximated by three rigid links (green colour) configurations. (c) The tail mechanism without its covering shows an increasing amplitude of the segments towards the peduncle

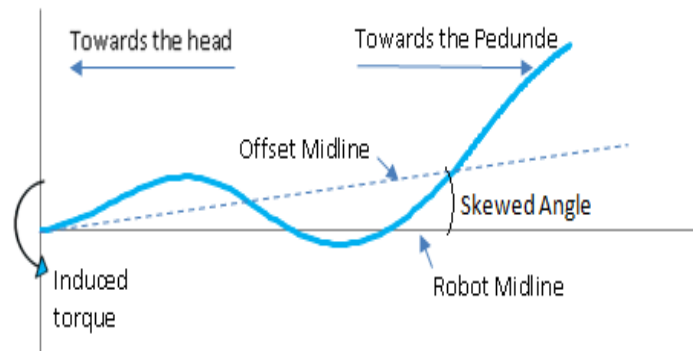


Figure 5: Lopsided traveling wave

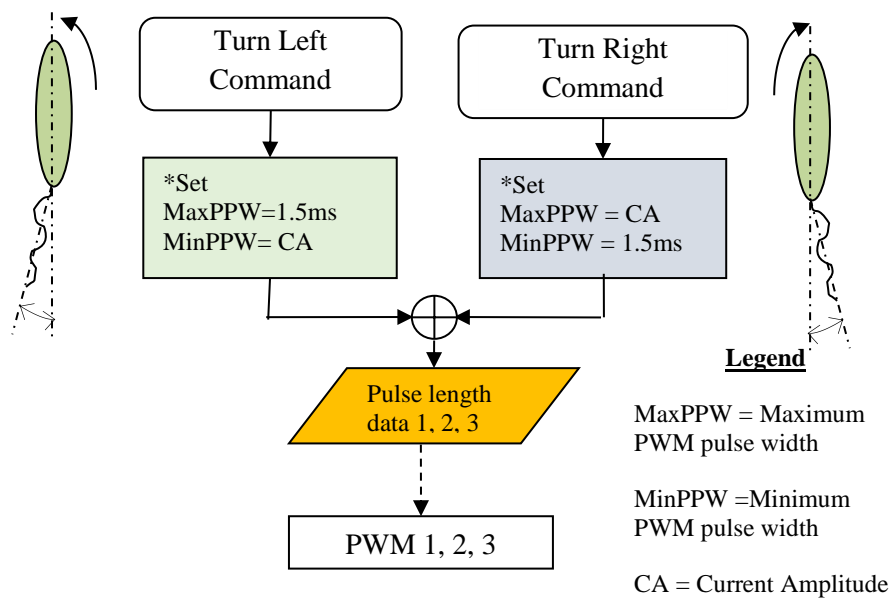


Figure 6: Turning routine

Algorithm for sharp-turning

The sharp turning involves sudden turning to either side as used by biological fishes for escaping predators. It involves bending suddenly in the direction of interest and forming a curve round about an imaginary cylinder, but with an increased radius of curvature from the tail towards the head, and then uncoils the tail (the flexible portion) rapidly after some moment as depicted in Figure 7. On the flowchart (Figure 8), the first action is saving the critical system data such as current pulse length data, amplitude data, etc into a designated register. Thereafter, how long the robot should coil is set, the amount of time to remain coiled is dependent on the current oscillation speed; high speed means lesser time to remain coiled. Next is the preparatory stage which involves making the robot to be straightened up by setting all the PWM pulse length to 1.5ms and then setting it to about 1ms for left-turning or 2ms for

right-turning, this will make the robot to have a curvature in the desired direction. The motor closest to the haul acts first, thereafter the middle motor and then the motor controlling the peduncle. The robot remains in this posture for the already set delay time. This delay is essential to this turning routine, the sudden curving process creates a circular momentum that reorients the robot. The uncoiling process thereafter follows. The uncoiling motion is in reverse order (the motor controlling the peduncle acts first, thereafter the middle motor and finally the motor driving the segment closest to the haul) after a fixed delay in time. In this manner, the robot peduncle act as a paddle which creates a drag during the coiling process, however during the uncoiling process, the head/haul inertial will cause the robot to stay in place in the direction turned to, while the tail changes its orientation to complete the turning.

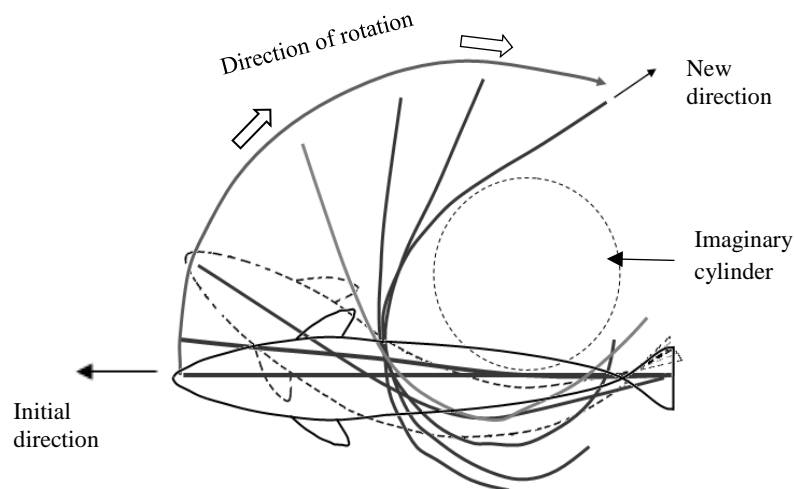


Figure 7: Sharp turning behavior of Mackerel (*Scromber scrombus*)

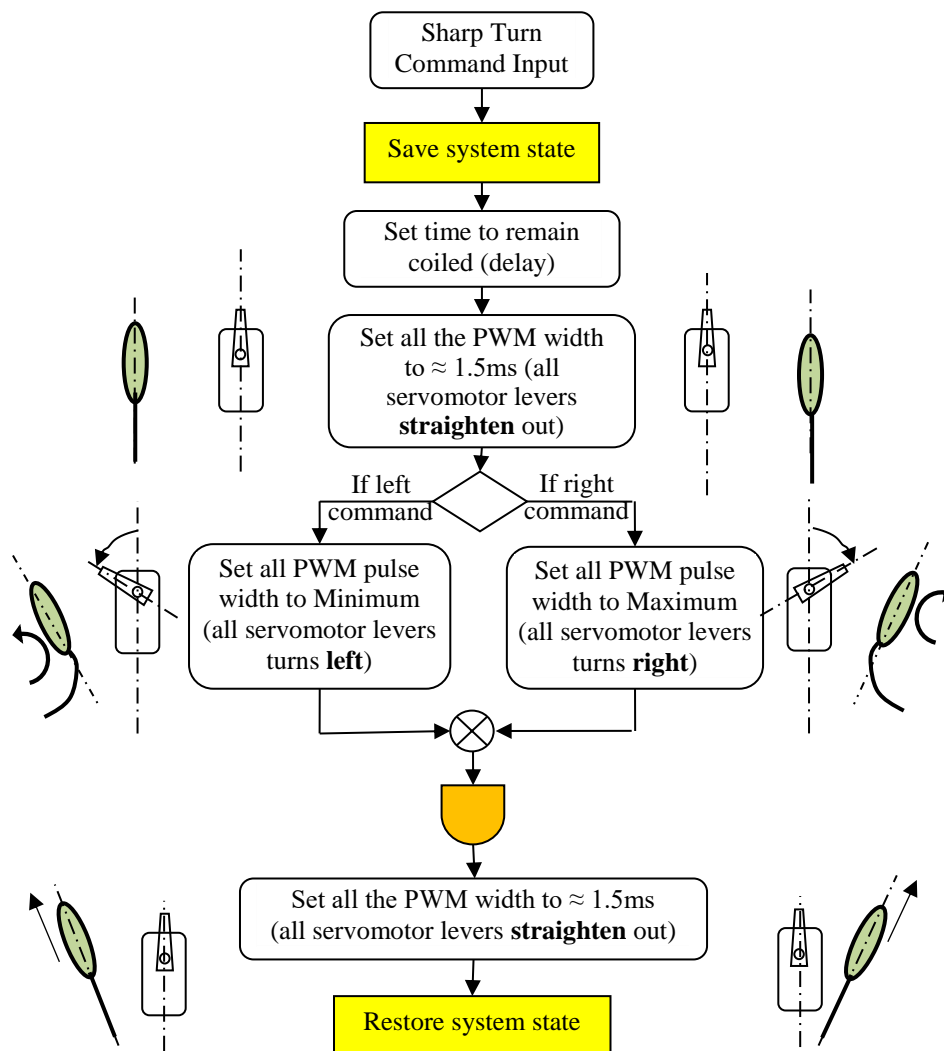


Figure 8: Flowchart for sharp turning algorithm

Experimental Verifications

The presented algorithms were verified by performing laboratory tests on the algorithms (that is with the robot out of

water) and then field tests. For the laboratory tests, the behaviour of the firmware for offset traveling wave pattern generation and sharp bending/ coiling shape routine were run

while the command to change swim directions or perform sudden change in direction of swimming was issued through a remote-control interface. The field tests were performed by placing the robot inside water pool for steady turning while swimming and wooden water tank for sharp turning. The pool has a depth range of 25cm to 50cm (equivalent pressure head of 2.4kPa – 4.9kPa) and the water tank dimension is 61cm x 122cm x 61cm filled with water to a depth of 30cm or pressure head of 2.91kPa.

For all the experiments, a Sony Cyber-shot digital camera (model DSC-S730) was used for recording the videos of the experiments. It has a resolution of 3 megapixels, F-stop of f/2.8, exposure time of 1/40 s, ISO speed of 100 and at 30 fps. Still images and time stamp were extracted from the recordings using Microsoft Windows Live™ Movie Maker Version 2011 with up to 10ms resolution in the interval between the still images.

RESULTS AND DISCUSSION

The offset traveling wave pattern for steady-turn algorithm

This is demonstrated in Figure 9. The robot is swimming normally from frame 1-10 and at frame 11, it receives a command to do offset swimming to the right side. So from frame 12 to 36, it restricted its tail oscillations to the midline and its right side. Frame 24 and 36 shows the constraint where the tail is forced to stop at the midline. 2 complete cycles were executed from frame 12 -36 before a restore to normal swimming command was received again at frame 37. Figure 10 is a graphical representation of what happened within the 51 frames of Figure 9.

The sharp-turn algorithm

This algorithm output is shown in figures 11a and 11b (the tail direction and constraints during the sharp turning routine). Frames 1- 16 and 28-36 are the normal swimming mode. At frame 17, the tail motion controller receives a command to perform left sharp turn, thereafter, it abandons the normal swimming mode and reverses its direction (frames 18 and 19).

It remains paused in that position for approximately 0.4s (frames 20-23). A fast return was then initiated (uncoiling) from frame 24 to 26 (within ~0.3s). At frame 27, the algorithm transits from the sharp turn to the normal swimming mode. Of note in Figure 11b is the overshoot at frame 19. The system was not tuned and its effect on the sharp turn was not investigated in this work. Also, at frame 28, the motion was not properly restored; this could be a programming error or timing error due to the acceleration at points 24 to 26. Jindong and Huosheng (2007) presented a thorough theoretical basis for the sharp turning of fishes, but the actual implementation shows a very poor outcome as obtained in this work too.

Steady turning while swimming – field testing

A steady turning to the left while swimming is demonstrated in Figure 12. The label on each frame shows the robot posture relative to the datum (the edge of the pool as shown in the first frame). The turning radius at this instance was measured approximately as 54cm and at a linear speed of 8.26cm/s (0.21 body length per second).

Sharp turning while swimming – field testing

The sharp turn command was activated by a bump sensor as described by Afolayan *et al.*, (2014), located at the head of the robotic fish while the robot swims inside a 61x122x61 cm³ wooden box filled with water up to a depth of 30cm. In Figure 13, the robot swims normally from frame 1-4 and then hit its head with the wall of the box at frame 5. Thereafter, the sharp turn procedure (to the left) was executed in frame 6. It was repeated after hitting its head against the wall first in frame 6 till the 12th frame. At frame 13-15, it has successfully turned. The small box allows this procedure to be repeated continuously until it no longer hit its head against the box side. The box width to fish length ratio is $\approx 3:2$. Similar to Marchese *et al.* (2014) and Li *et al.* (2018) works, the sharp turning is still not at the same speed as that of a living fish. In both works, the turning was even enhanced with hydraulic flow/jet (Marchese *et al.*, 2014)) and pectoral fin (Li *et al.*, 2018).



Figure 9: Right offset swimming mode; frame interval is 0.1s

Legend

- Left to right motion
- ← Right to left motion
- ←⊖ Start skewed motion
- ⊙ Stop skewed motion
- ┌→ Left to right motion but restricted to right half of the robot
- └← Right to left motion but restricted to right half
- Tail motion constrained not to exceed the midline

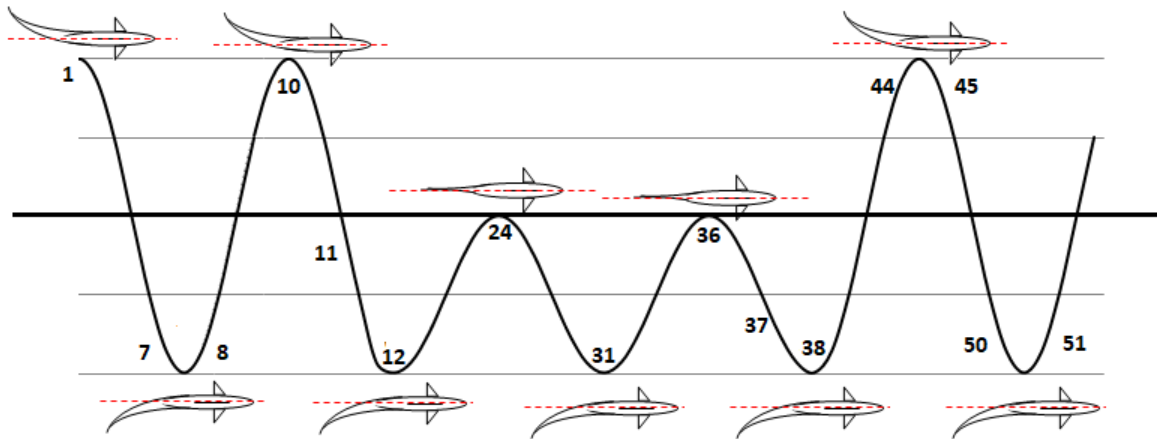


Figure 10: Tail displacement for right offset swimming mode. The numbers represent an equivalent position in Figure 9.



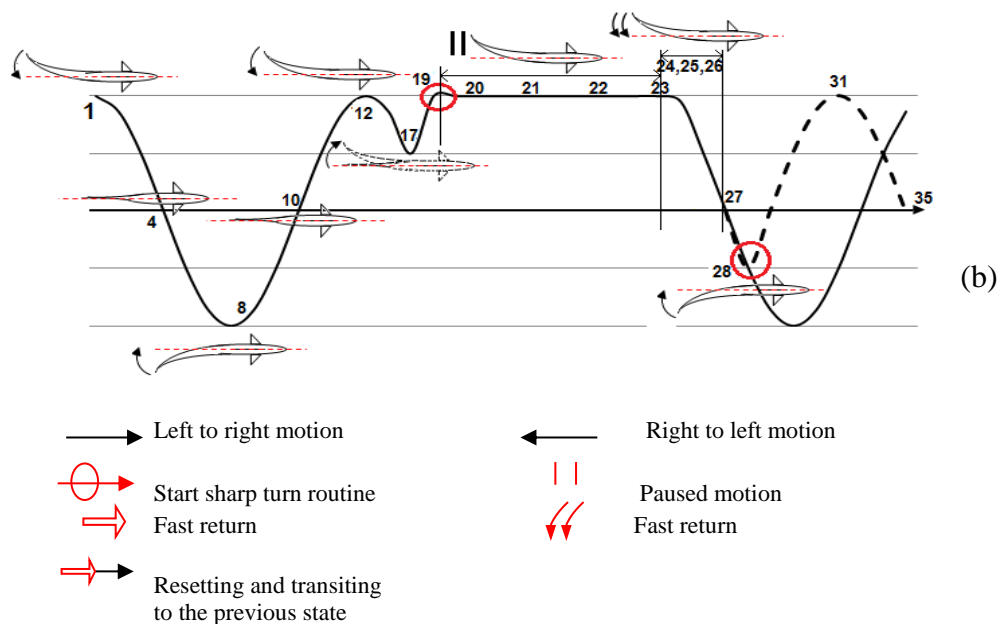


Figure 11: The robot executing the left sharp turn algorithm. The numbering in (b) corresponds to that in (a)

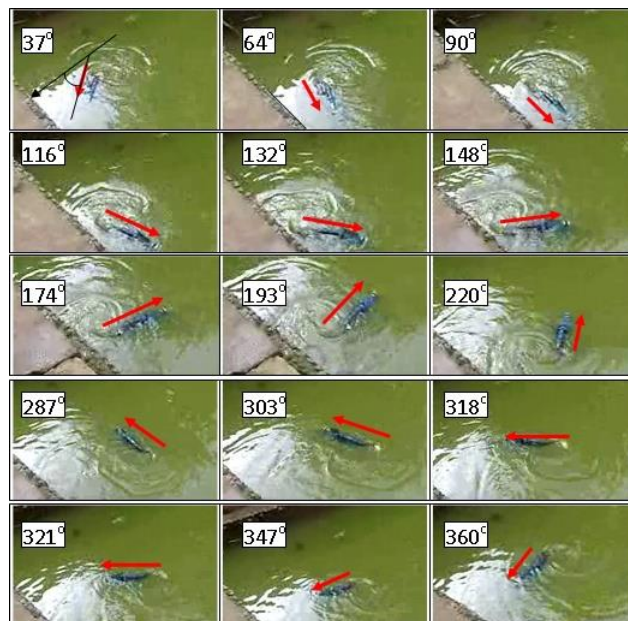


Figure 12: The robot makes a circular turn leftward while steadily swimming. The frame interval is 1.2s.

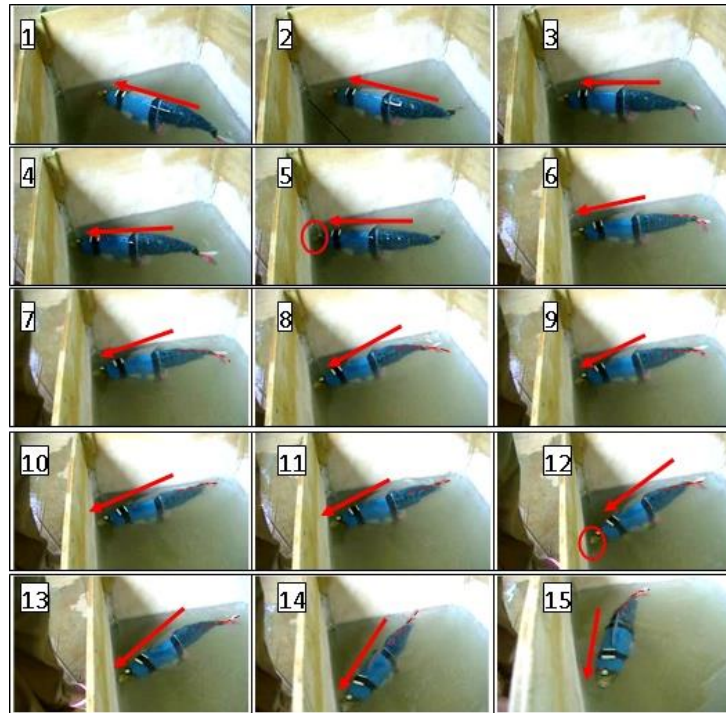


Figure 13: A sharp turn is demonstrated in a box filled with water

CONCLUSIONS

Two biomimetic underwater robot direction changing algorithms presented in this work was based on an inflexible but less computational demanding design called built-in patterns for its motor and motion control scheme. The steady-turning while swimming algorithms performed as designed with a turning radius of 54cm while the other algorithm – sharp-turn works also but not as desired. The second algorithm limitation is due to the mechanical structure of the robotic fish and the untuned or unoptimized control parameters of the robot components, such as the motor delay, motor and gear inertial. It is recommended that the tuning be performed on subsequent developed robot so that the sharp-turn can mimic a real biological model or even exceed it

FUNDING

This project was supported by the MacArthur Foundation Thesis Completion Grant.

REFERENCES

Afolayan, M. O., Yawas, D. S., Folyan, C. O., & Aku, S. Y. (2012). Mechanical Description of a Hyper-Redundant Robot Joint Mechanism Used for a Design of a Biomimetic Robotic Fish. *Journal of Robotics*, 2012, 1-16.

Afolayan, M. O., & Iorpenda, M. J. (2021). Plain Swimming Algorithm for a Mackerel (*Scomber scombrus*) Robotic Fish. *Nigerian Research Journal of Engineering and Environmental Sciences*, 6(2) 2021 pp. 783-793.

Afolayan, M.O., Yawas, D. S., Folyan, C. O., & Aku, S.Y. (2014) A Design of Bump Sensor Mechanism for Robotic Fish. *British Journal of Applied Science and Technology* 5(6): 568-579. 2015

Andrés, M., Juan, J. R., Iván R., Jaime del C., & Antonio, B. (2020). Design of a Hyper-Redundant Robot and Teleoperation Using Mixed Reality for Inspection Tasks. *Sensors*. 20(8), 2181, DOI:10.3390/s20082181

Anderson, J. M. (1996). *Vorticity control for efficient propulsion*. Ph.D. dissertation, Massachusetts Institute of Technology/Woods Hole Oceanographic Institute Joint Program, Woods Hole, MA.

Breder, C. M. (1926). The locomotion of fishes. *Zoological*, 4, 159–297.

Daou, H. E., Salumae, T., Toming, G., & Kruusmaa, M., (2012). A bio-inspired compliant robotic fish: Design and experiments. In *IEEE International Conference on Robotics and Automation* (pp. 5340-5345). Saint Paul, MN, USA., doi: 10.1109/ICRA.2012.6225321.

Jindong, L., & Huosheng, H., (2007). A methodology of modelling fish-like swim patterns for robotic fish. In *Proceedings of the 2007 IEEE International Conference on Mechatronics and Automation* (pp. 1316–1321). Harbin, China.

Kevin, J. D. (1997). *Limbless locomotion: learning to crawl with a snake robot*. A Ph.D. thesis at the Robotics Institute Carnegie Mellon University, 5000 Forbes Avenue, Pittsburg, PA 15213.

Li, Z., Ge, L., & Xu, W. (2018). Turning Characteristics of Biomimetic robotic fish driven by two degree of freedom of pectoral fins and flexible body/caudal fin. *International Journal of Advanced Robotic Systems*. 2018: 1-12

Logico, M. G. (2006). “Navy Diver Sets Record with 2,000 foot Dive”, <http://www.military.com/features/0,15240,108883,00.html>. Accessed: 18-May-2022.

Marchese, A. D., Onal C. D., & Rus, D. (2014). Autonomous Soft Robotic Fish Capable of Escape Maneuvers Using Fluidic Elastomer Actuators. *Soft Robotics*, 1(1), 75-87.

- Mark, C. (2021). Advances in underwater robots. <http://www.asme.org/topics-resources/content/advances-in-underwater-robots>. Accessed: 04-June-2022
- Martins, O. O., Aribisala, A. A., Adeyemi, H. O., Adekunle, A. A., Oyelaran, O. A. (2019). Dual Mode Mobile Surveillance Robot. *FUDMA Journal of Sciences (FJS)*, Vol. 3 No. 4, December, 2019, 153-162.
- Müller, U., Heuvel, B., Stamhuis, E., & Videler, J. (1997). Fish foot prints: morphology and energetics of the wake behind a continuously swimming mullet (*Chelon Labrosus Risso*). *Journal of Experimental Biology*, vol. 2906, pp. 2893–2906.
- NMRI (2020). National Maritime Research Institute. <http://www.nmri.go.jp/oldpages/eng/khirata/fish/>. Accessed 04 July, 2020.
- Salisu, A., Bugaje, A. and Shallah, A.B. (2020). Line following Robot with Hugh Radiation Material Detection Capability. *FUDMA Journal of Sciences (FJS)*, Vol. 4 No. 4, December, 2020, 274-280. DOI: <https://doi.org/10.33003/fjs-2020-0404-482>.
- Salumäe, T. (2014). *Flow-Sensitive Robotic Fish: From Concept to Experiments*. PhD Dissertation Submitted to Faculty of Information Technology, Centre for Biorobotics, Tallinn University of Technology, Tallinn, Estonia
- Salumäe, T., & Kruusmaa, M. (2011). A Flexible Fin with Bio-Inspired Stiffness Profile and Geometry. *Journal of Bionic Engineering*, vol. 8, no. 4, pp. 418–428.
- Sfakiotakis, M., Lane, D. M., & Davies, J. B. C. (1999). Review of fish swimming modes for aquatic locomotion. *IEEE Journal of Oceanic Engineering*, 24, 237–252.
- Shugen, M.A., & Mitsuru, W. (2002). Time-optimal control of kinematically redundant manipulators with limit heat characteristics of actuators. *Advanced Robotics*, Vol. 16. No. 8. pp. 735-749 (2002).
- Srinivasan, M. V. (1992). Distance Perception in Insects. *Centre for Visual Sciences, Research School of Biological Sciences, Australian National University, Australia*. pp 1-10. Cambridge University Press.
- Streitlien, K., Triantafyllou, G. S., & Triantafyllou, M. S. (1996) Efficient foil propulsion through vortex control. *American Institute of Aeronautics and Astronautics Journal*, 34, 2315–2319.
- Than, K. (2012). James Cameron Completes Record-Breaking Mariana Trench Dive. <http://www.nationalgeographic.com>. Accessed:18-May-2022
- Wang, T., Wen L., Liang J., & Wu, G. (2010). Fuzzy vorticity control of a biomimetic robotic fish using a flapping lunata tail. *Journal of Bionic Engineering*, 7, 56–65.
- Watson, D. G. M. (2002). *Practical ship design*, vol. 1. Gulf Professional Publishing.
- Yangwei, W., Jinbo, T., & Dongbiao, Z. (2015). Design and Experiment on a Biomimetic Robotic Fish Inspired by Freshwater Stingray. *Journal of Bionic Engineering*, 12, 204–216.



©2022 This is an Open Access article distributed under the terms of the Creative Commons Attribution 4.0 International license viewed via <https://creativecommons.org/licenses/by/4.0/> which permits unrestricted use, distribution, and reproduction in any medium, provided the original work is cited appropriately.